J Solid State Electrochem (1998) 2: 386–393

ORIGINAL PAPERS

Maheshwar Sharon · Youn-Seoung Lee
Chung-Nam Whang · Susanta Ghosh

Effect of platinum on the photoelectrochemical behavior of lead oxide thin film

Received: 19 November 1997 / Accepted: 9 March 1998

Abstract The effect of Pt on the photoelectrochemical behavior of lead oxide prepared from anodization of Pb-Pt alloy containing various concentrations of Pt has been studied. It is observed that, while Pt reduces the resistivity of the oxide film, it also reduces the photoconversion efficiency of the photoelectrochemical cell prepared from this material. The reason for this low efficiency is discussed.

Key words Lead oxide · Pt doping · Gartner model · Photoelectrochemical cell

Introduction

Anodization of lead in sulfuric acid is known to give a photoactive PbO with a band gap energy of 1.92 eV [1, 2]. Sharon et al. [3–8], on the other hand, synthesized photoactive PbO by potentiodynamic oxidation of lead in alkaline solution and studied its photoelectrochemistry in alkaline medium. Though the open-circuit photopotential (around 800 mV) obtained with this material is reported to be better than that of a silicon solar cell, its short-circuit photocurrent is found to be in the vicinity of 1–4 mA cm^{-2}. Two reasons have been suggested for the low photocurrent: (1) high resistance of the pure PbO and (2) difficulties in growing PbO with a highly developed (110) plane (this plane is reported to be responsible to show photoactivity in PbO). Minoura et al. synthesized α-PbO thin film with a highly oriented (110) plane by potentiostatic oxidation of lead at 0.3 V vs SCE [9] in alkaline medium. This could yield the photocurrent up to 4.3 mA cm^{-2}. Sharon et al. [10, 11] slightly improved the conductivity of PbO film by potentiodynamically oxidizing lead alloy made from tin and indium. The result was, however, not very encouraging. Since platinum has been reported to help in photocatalyzing the surface of CdS and thus enhancing the photocurrent [12], it was purposed to make an alloy of lead and platinum with different percentages of platinum and to anodize the lead alloy to obtain platinum-doped PbO.

In this paper, we report the effect of platinum on the photoelectrochemical behavior of lead oxide anodized from alkaline solution under potentiodynamic conditions from Pb-Pt alloy containing different concentrations of platinum.

M. Sharon (✉) · S. Ghosh
Department of Chemistry, Indian Institute of Technology, Bombay, Powai, Mumbai, 400 076, India
e-mail: sharon@chem.iitb.ernet.in

Y.-S. Lee · C.N. Whang
Department of Physics, Yonsei University, Seoul 120-749, Korea

Experimental

The Pb-Pt alloy electrodes were prepared by melting Pb (purity 99.999%, BDH) and pure platinum in the required proportion at 600 °C under vacuum (10^{-3} to 10^{-4} Pa) in a quartz tube for 7 days and then cooled by dropping the capsule in the liquid nitrogen. From the rod-shaped alloy small pieces were cut and flattened to 1 mm thick foil with the help of hydraulic press. Electrodes of 1 cm^2 area were made from such foils as discussed elsewhere [4]. The exposed lead surfaces were then polished with a 1000c carborundum paper.

The electrochemical cell consisted of a three-electrode setup. Pb-Pt alloy electrode of area 1 cm^2 was used as a working electrode. A platinum foil (4 cm^2) and a normal Hg/HgO (0.12 V vs NHE) electrode were used as a counter and a reference electrode, respectively. 0.1 M NaOH prepared in 0.1 M Na_2SO_4 solution was used as an electrolytic bath to synthesize α-PbO. Before anodic oxidation, the Pb-Pt alloy electrode was etched with a mixture of methanol, glacial acetic acid and hydrogen peroxide (1:1:1), washed with double-distilled water and then kept in the electrolyte at 80 °C (Toshniwal Instruments, India). Potentiodynamic anodization of Pb-Pt alloy electrode was carried out at different potential regions for different time intervals. The films obtained after 20 min of anodization at a sweep rate of 100 mV s^{-1} in the potential range from −0.2 V to +0.2 V (vs Hg/HgO) gave the best photoresponse. After anodization, the electrodes were washed thoroughly with double-distilled water and kept at 130 °C for 1 h in a vertical furnace fitted with an external temperature controller (ULVAC,

HPC 7000). The XRD patterns of the oxide films were recorded using an X-ray diffractometer (Philips, model PW 1810) with Cu-K_α radiation. The surface morphology and the composition of the oxide films were observed with a scanning electron microscope (Cameca SU 30) and ESCA, respectively.

A photoelectrochemical (PEC) cell of the configuration α-PbO doped Pt|0.1 M $Fe(CN)_6^{-3/-4}$| Pt was constructed. The experimental setup for measuring the photocurrent consisted of the following units: stabilized 100-W tungsten-halogen lamp, monochromator (Action Research Corporation, model 150, USA), light chopper (PAR, model 197, USA), lock-in analyzer (PAR Model-5204, USA), potentiostat/galvanostat (PINE Model-AFRDE4, USA) and the PEC cell. The action spectra were normalized with the help of a calibrated silicon photodetector.

Results and discussion

Cyclic voltammetric studies of Pb-Pt alloy electrodes

In order to confirm the potential responsible for the oxidation and reduction process of platinum present in the Pb-Pt alloy, cyclic voltammetric studies of electrodes with different concentrations of Pt were performed in the potential range −1.25 V to +2.35 V vs Hg/HgO (Fig. 1). Barring two new peaks due to Pt → PtO (A_3) and PtO → Pt (C_3), cyclic voltammograms (CVs) of all electrodes were similar [7]. However, peaks for platinum were apparent only with higher concentration of Pt in Pb (i.e. >5 wt%). The anodic peaks A_1 and A_2 are due to oxidation of Pb → PbO and PbO → PbO_2, respectively. The cathodic peaks C_1 and C_2 are due to PbO_2 → PbO and PbO → Pb, respectively.

A potentiodynamic anodization of Pb-Pt alloy electrode was carried out in the range −0.2 V to +0.2 V (vs

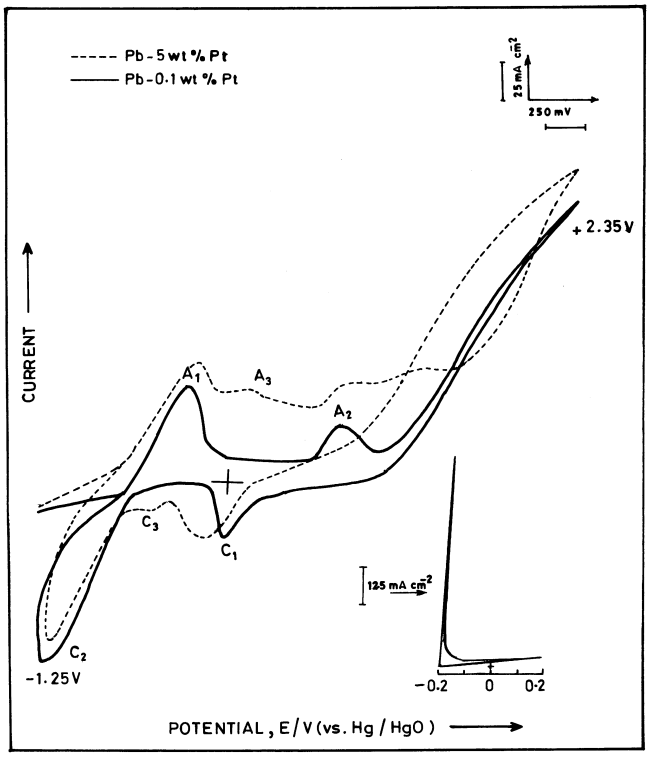

Fig. 1 The cyclic voltammogram for potentiodynamic anodization of *a* Pb/0.1 wt% Pt (*continuous line*) and *b* Pb/5 wt% Pt electrodes (*broken line*) in 0.1 M NaOH solution at 80 °C (sweep rate) 100 mV s^{-1}), electrode area 1 cm^2. The inset shows the CV for −0.2 V to +0.2 V

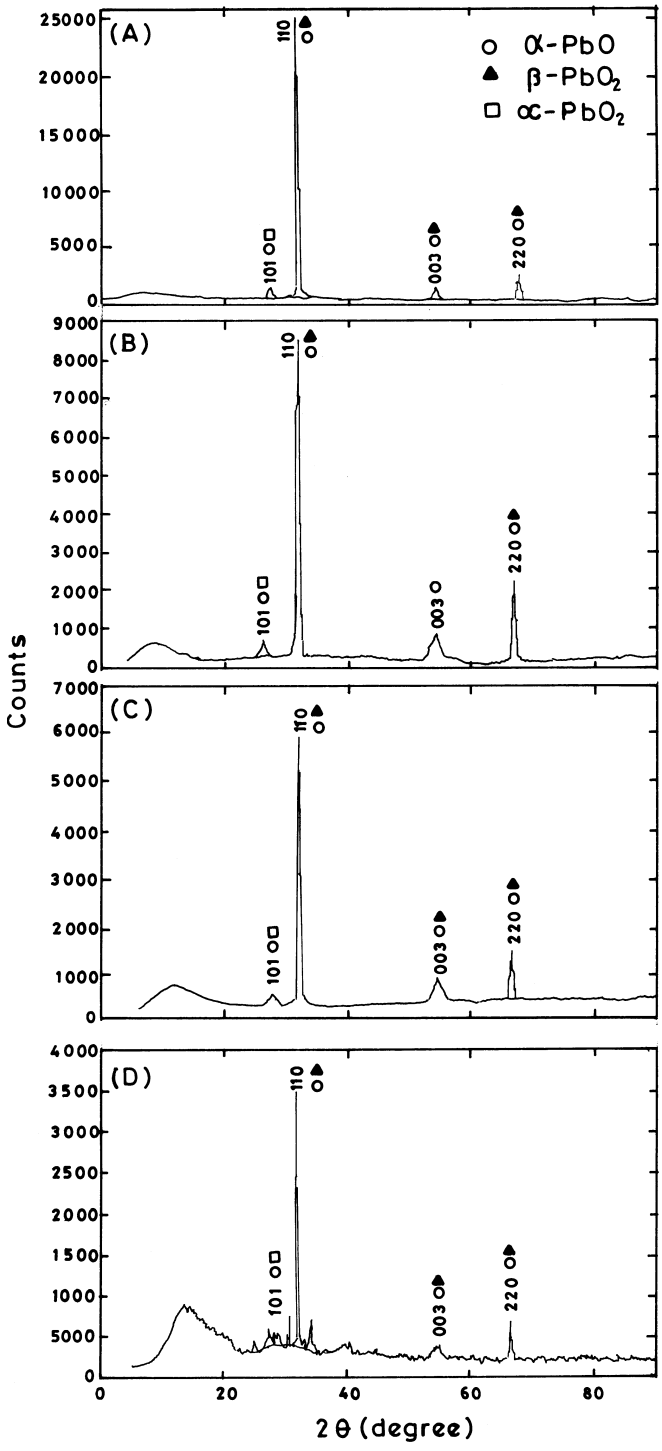

Fig. 2A–D The XRD pattern of Pb/X wt% Pt oxide film **A** $X = 0.0$, **B** $X = 0.1$, **C** $X = 1.0$ and **D** $X = 5.0$ obtained by the potentiodynamic technique in the potential region of −0.2 V to +0.2 V vs Hg/HgO

Hg/HgO) (inset of Fig. 1 shows the CV for this region), because −0.2 V is the overpotential for PbO formation and +0.2 V is slightly greater than the onset potential for PbO_2 formation but high enough to allow the growth of PbO. The range of potentials (A_3 or C_3) corresponding to Pt ⇌ PtO was not used, because it might have formed PbO enriched with PbO_2. Hence, the anodization of Pb-Pt alloy in this range would not form PtO while growing PbO thin film. In other words, platinum present in the anodized PbO film obtained from the anodization of Pb-Pt alloy is expected to be present in its metallic form.

X-ray diffraction studies

The XRD pattern of oxide films obtained from Pb-Pt alloy containing different wt% of Pt (recorded from Philips model PW 1810 with Cu-K_α radiation) after 20 min of anodization is shown in Fig. 2. The intensity of the major peak corresponding to the plane (110) seems to decrease as the concentration of platinum increases in the Pb-Pt alloy. Moreover, this plane has been shown to be responsible for the photoactivity in α-PbO film [9]. This suggests that, with the increase in Pt concentration, the photoactivity of the α-PbO should decrease. Apart from this plane, it appears that Pt concentration does not have much influence on the growth of other planes of α-PbO. Since *d*-values for α-PbO and β-PbO_2 are very close to each other (Fig. 2), it is difficult to ascertain their presence by XRD alone [13]. No XRD peaks corresponding to Pt, PtO or PtO_2 were observed, though a hump below $2\theta = 20°$ seems to grow as the concentration of Pt increased in Pb-Pt alloy. However, it is obvious that, though XRD peaks corresponding to Pt or its oxide are not observed, Pt has certainly suppressed the growth of plane (110) of α-PbO.

Parameters of the α-PbO unit cell formed with Pb-Pt alloy, containing different wt% Pt, were calculated with the help of standard XRD software and compared with the standard data obtained from pure lead. These calculations suggest (Table 1) that as the concentration of Pt is increased in Pb-Pt alloy, the unit cell dimension of α-PbO as well as the volume of its unit cell decreases. In other words, there is a contraction in the cell dimension with increase in Pt concentration in Pb-Pt alloy. This may be the reason for the increase in the conductivity of the α-PbO films obtained with Pb-Pt alloy. It will be seen later that in spite of increasing conductivity of the film (as observed in Mott-Schottky studies), the photocurrent decreased with increase in Pt concentration in Pb-Pt alloy because of the suppressed growth of the plane (110). It is interesting to observe that platinum in Pb-Pt alloy behaves similarly to Sn or In in Pb-Sn or Pb-In alloys [10, 11], suggesting that, like Sn or In, Pt also destroys the formation of the (110) plane.

The crystal size was obtained from the full-width half-maximum of the XRD peak by using the following equation [14, 15];

$$D = \frac{\lambda}{\beta \cos\theta} \tag{1}$$

where β is the full width half maximum, λ is the wavelength of X-rays (1.5406 Å) and D is the average crystal size (Table 1).

Raman aspectroscopic study

In order to confirm the different phases present in the oxide film, a Raman spectroscopic study was carried out. Figure 3 shows the Raman spectra of lead oxide films obtained by the anodization of pure lead and Pb-0.1 wt% Pt alloy, respectively. It was found that a major line appeared at 155 cm^{-1} with a complementary line at 350 cm^{-1} for α-PbO, whereas the complementary line at

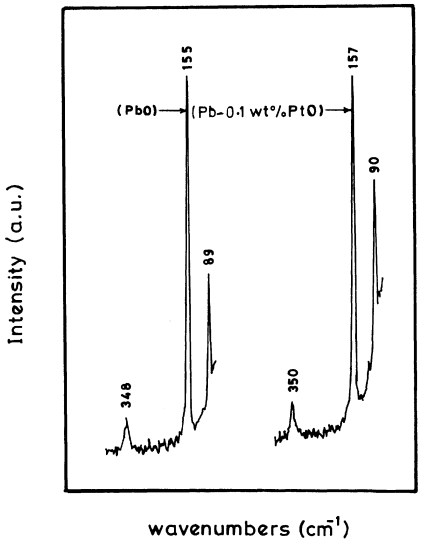

Fig. 3 Raman spectrum of the oxide films grown on Pb and Pb/0.1 wt% Pt substrate

Table 1 Cell parameters, flat-band potential and donor density

Wt% Pt	*a* (Å)	*c* (Å)	*v* (cm^3)	Crystal size (Å)	V_{fb} (*V* vs SCE)	N_d (cm^{-3})
0.00	3.9703	5.0350	79.37	660	−0.65	5.77×10^{15}
0.10	3.9559	5.0787	79.48	268	−0.64	1.12×10^{17}
1.00	3.9308	4.933	76.22	188	−0.62	3.01×10^{20}
5.00	3.9320	4.98	76.99	176	−0.60	6.39×10^{20}

288 cm^{-1} for β-PbO [16] was absent. This experiment has thus confirmed the presence of α-PbO. Presence of PbO_2 could not be ascertained as this phase is Raman inactive [16].

X-ray photoelectron spectroscopic study

The XPS study was carried out to confirm the presence of platinum in the lead oxide film. The XPS spectrum of the alloyed Pb-0.1 wt% Pt oxide film obtained after 20 min of potentiodynamic anodization is shown in Fig. 4. The core-binding energy of Pb $4f_{7/2}$ and O 1 s states are 138.25 eV and 529.6 eV, respectively. The binding energy difference between the two states is 391.35 eV, which is very close to the reported value for α-PbO (391.5 eV) [17–19]. The slight difference may be due to the nonstoichiometry of the oxide film. The core-binding energies of Pt $4f_{7/2}$ and Pt $4f_{5/2}$ are 71.2 eV and 74.53 eV, respectively. The difference in binding energy between two states is 3.33 eV, which corresponds to pure platinum [12]. Therefore, the presence of platinum in the oxide films can be expected, and it should also be in the metallic form. The higher energy level for O 1 s is observed in the surface of the oxide films, and this is due to the presence of undesired lead hydroxide on the surface, which might have been formed during the anodization in the alkaline medium.

Figure 5 shows the depth profile spectrum of the oxide film. The depth profile of the oxide film was studied using Ar as the etchant, and the sputtering rate was kept at

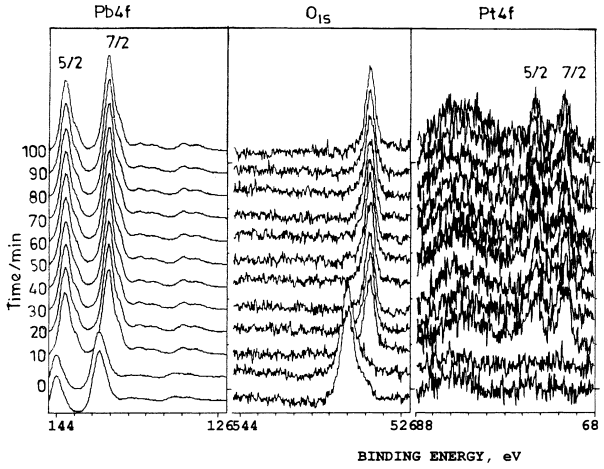

Fig. 4 The binding energy values of $Pb4f_{7/2}$, $Pb4f_{5/2}$ and O 1s states after each 2 min of sputtering with Ar ion for Pb/0.1 wt% oxide (sputtering rate is 10 Å min^{-1})

10 Å min^{-1}. The ratio of O to Pb^{2+} is calculated up to a depth of 100 nm and found not to be constant. The average ratio is 0.75. This means that film is oxygen deficient. The variation of O/Pb^{2+} ratio is due to

Fig. 5 The depth profile spectrum for the concentrations of oxygen and lead in the oxide film (Pb/0.1 wt% oxide) in terms of sputtering time; sputtering rate 10 Å min^{-1}

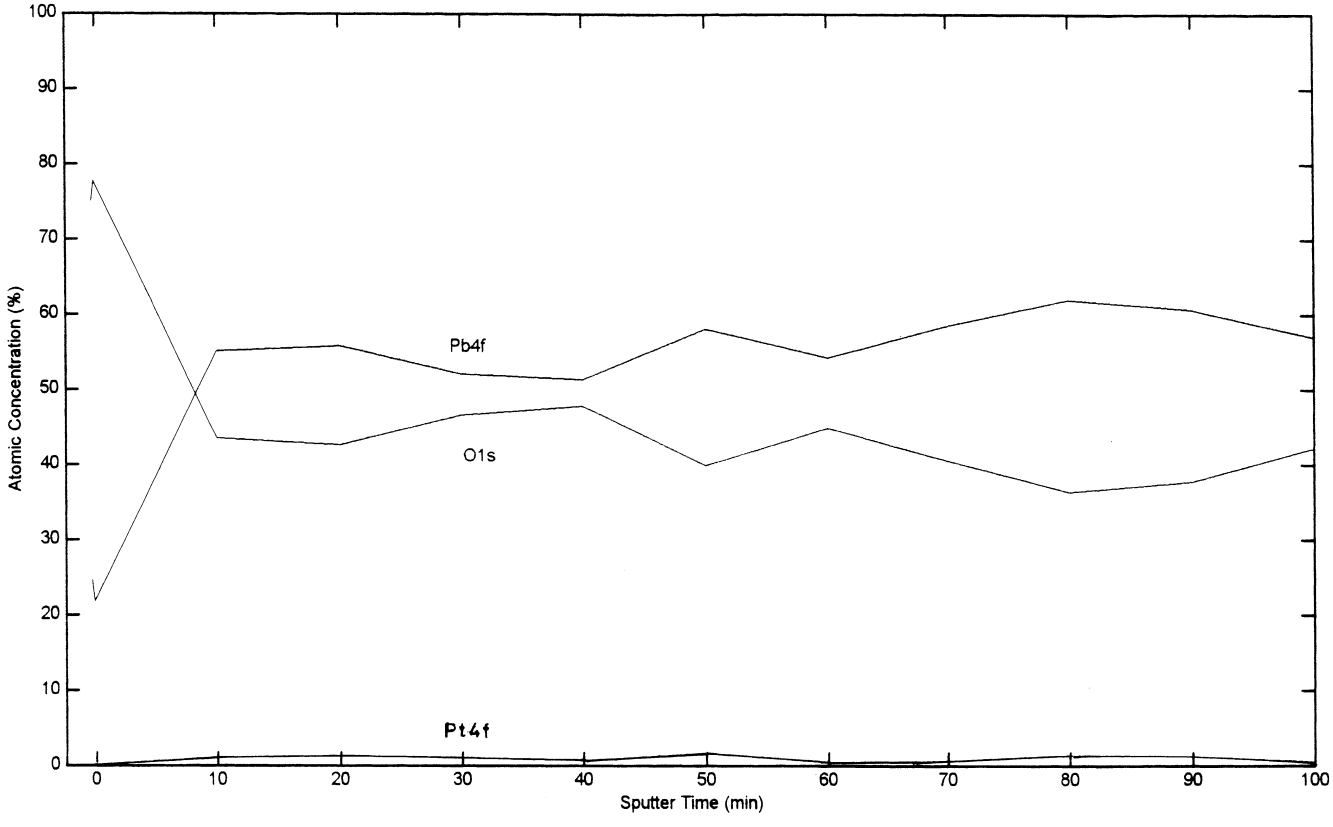

nonhomogeneity of Pb-Pt alloy. XPS study thus reveals that platinum is controlling the O/Pb^{2+} ratio in the film.

SEM study

Figure 6a shows an SEM micrograph for Pb-0.1 wt% Pt alloy that was anodized in the potential range from −0.2 V to +0.2 V for 20 min. It was found that many micropores exist in the outer layer of oxide thin film. Figure 6b shows the cross-sectional view of Pb-0.1 wt% Pt oxide electrode anodized for 20 min. The thickness of the oxide film was found to be 10 μm.

Impedance study

The flat-band potentials of Pt-doped lead oxide films were obtained by using the Mott-Schottky (M-S) relation. The semiconductor electrolyte interface under dark condition has been modeled so that the surface states capacitance and space charge capacitance are placed in parallel [20]. A typical M-S plot for Pb-0.1 wt% Pt oxide electrode is shown in Fig. 7. The flat-band potentials for platinum-doped lead oxides were obtained from the intercept on the x-axis and the donor density was calculated from the slope of the plot. The results of the impedance study reveal that, as the concentration of platinum is increased, the donor density increases, whereas the flat band potential decreases (Table 1).

Since XPS study has revealed that platinum seems to control the ratio of O/Pb^{2+}, one could conclude that incorporation of platinum in the alloy might also be increasing the oxygen deficiency in the α-PbO film. Moreover, since the crystal dimension decreases with increase in platinum concentration (as revealed from the XRD analysis), one may also conclude that platinum might be influencing the band positions of the α-PbO and hence the Fermi energy. If this be so, it would be interesting to study the ultra-violet photoelectron spectroscopy (UVPS) of these films to confirm the variation in the Fermi energy with platinum concentration. In the absence of this facility, we are unable to take up this study.

Photoelectrochemical studies

The photoelectrochemical study was carried out using a large-area Pt counter electrode and a lead oxide semiconductor as working electrode. 0.1 M $Fe(CN)_6^{-3/-4}$ redox electrolyte was used for this purpose. The configuration of the PEC cell was thus oxide photoanode (1 cm^2) | 0.1 M $Fe(CN)_6^{-3/-4}$(pH9.2) | Pt (4 cm^2).

The band gaps of oxide electrodes were determined from the photoaction spectrum at different wavelengths and found to be 1.92 eV and 2.17 eV for indirect and direct transitions, respectively (Fig. 8) [4]. This reconfirmed that α-PbO is the main photoactive phase.

Quantum yield studies

The quantum yields of the above PEC cells were obtained under white light illumination [4]. A maximum

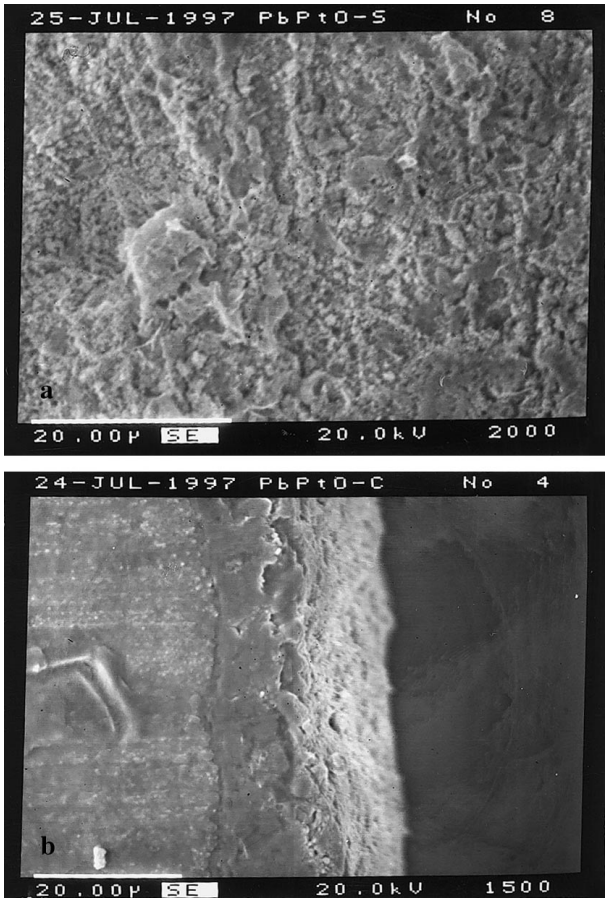

Fig. 6a, b SEM view of the oxide film showing **a** the surface morphology and **b** cross-sectional view of Pb/0.1 wt% Pt electrode

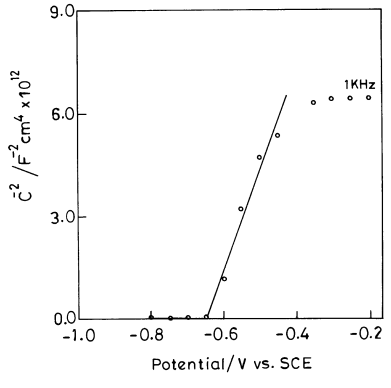

Fig. 7 Mott-Schottky plot of the oxide semiconductor over Pb/0.1 wt% Pt electrode in 0.1 M $Fe(CN)_6^{-3/-4}$ solution (pH 9.2, buffer)

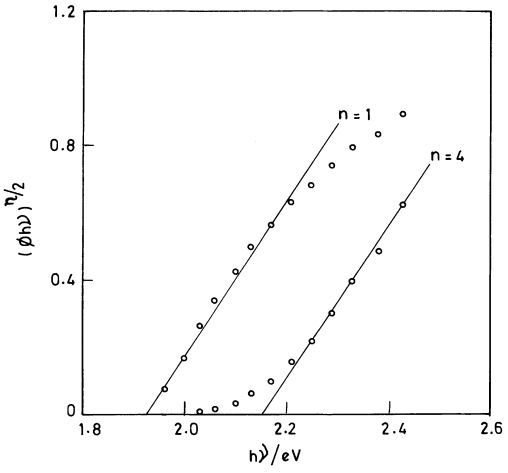

Fig. 8 $(\phi \times h\nu)^2$ vs $h\nu$ and $(\phi \times h\nu)^{1/2}$ vs $h\nu$ plots for measuring the band gap energy of the oxide film over Pb/0.1 wt% Pt electrode

quantum yield of 41.4% was obtained at 480 nm for Pb-0.1 wt% oxide, as shown in Fig. 9. A lower quantum yield (73% [9]) than for pure lead oxide was observed for platinum-doped lead oxide film. Suppression of growth of α-PbO along the (110) plane, as revealed from XRD results, might be one of the reasons for getting a low quantum yield.

Solar-to-electrical conversion

Figure 10 shows the power output curve for lead oxide obtained by anodization of pure lead and Pb-0.1 wt% oxide under the same optimized conditions. This result also confirms that, because of suppression of growth of the (110) plane of α-PbO, the photoactivity of lead oxide obtained with Pb-Pt alloy is lower than the photoactivity of lead oxide obtained with pure lead. Similar behavior was observed with Sn and In [10, 11].

Photocurrent quantum yield-potential relation

Though from the previous studies it is amply clear that platinum suppresses the growth of the (110) plane and hence decreases the photoactivity of the lead oxide film, it would also be equally interesting to find out whether platinum controls the formation of space charge width or diffusion region. For this purpose, Gartner analysis was carried out with lead oxide obtained with Pb-0.1 wt% Pt alloy. For the region where recombination of electron-hole pairs is prevented for an n-type semiconductor, a very useful relationship has been derived by Gartner [21, 22];

$$-\ln(1-\phi) = \alpha\left(\frac{2\epsilon\epsilon_0}{qN_d}\right)^{1/2}(V - V_{fb})^{1/2} + \ln(1+\alpha L) \qquad (2)$$

where terms have their usual meaning. The values of absorption coefficient (α) and diffusion length (L) can be obtained from the slope and intercept of the $-\ln(1-\phi)$ vs $(V - V_{fb})^{1/2}$ plot, knowing the donor density and the dielectric constant of α-PbO.

In order to use this equation, quantum yield versus the potential applied to the lead oxide electrode in a cell of configuration "Lead oxide photoanode (1 cm^2) |0.1 M $Fe(CN)_6^{-3/-4}$(pH9.2) | Pt (4 cm^2)" was measured by illuminating the lead oxide electrode with different wavelengths of light. Figure 11 shows the quantum yield vs potential plot for lead-platinum (0.1 wt%) oxide photoanode at different monochromatic wavelengths.

From the set of linear plots of $-\ln(1-\phi)$ vs $(V - V_{fb})^{1/2}$ in the region where electron-hole pair recombination is expected to be a minimum (limitation of the Gartner model) (Fig. 12), slopes and intercepts for each wavelength were calculated using the least-squares fit method, and values of α and L were calculated (Table 2) knowing the donor density from the a.c. impedance study (Table 1) and the dielectric constant (25.9) of α-PbO [23].

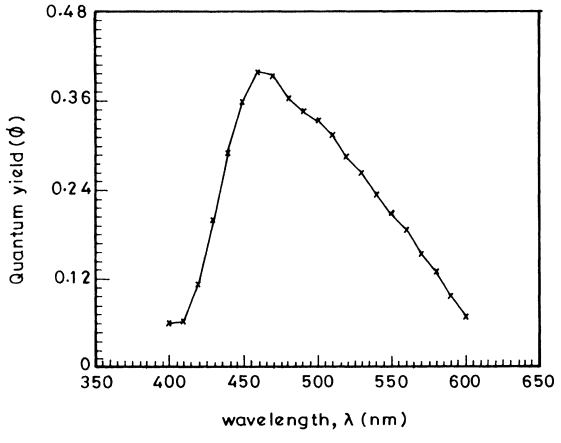

Fig. 9 Wavelength dependence of the quantum yield of the Pb/0.1 wt% Pt oxide photoanode after 20 min anodization

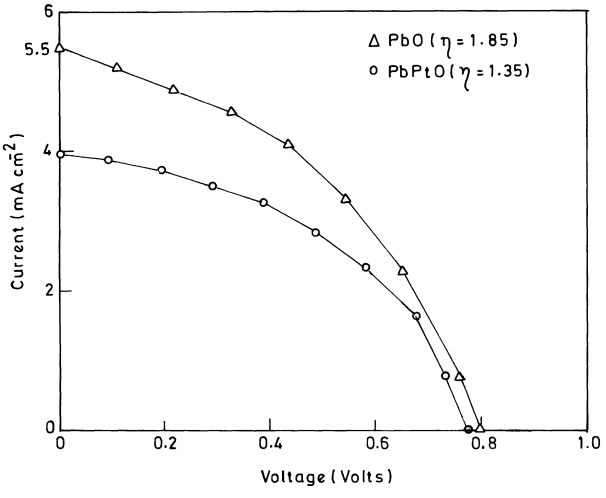

Fig. 10 Power conversion efficiency curve of Pb/0.1 wt% Pt oxide photoanode in 0.1 M $Fe(CN)_6^{-3/-4}$ solution (pH 9.2, buffer)

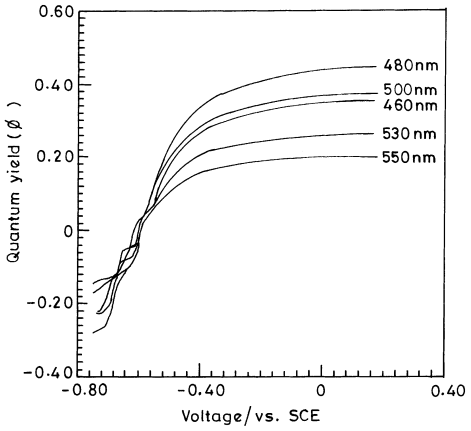

Fig. 11 Variation of photocurrent of Pb/0.1 wt% Pt oxide film with the applied bias under monochromatic illumination of various wavelength

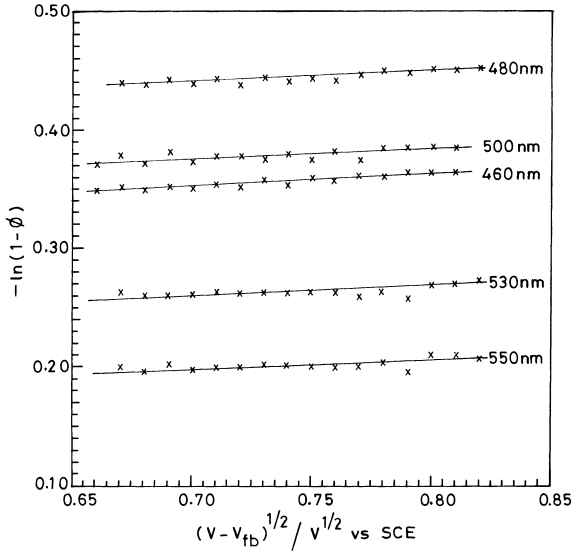

Fig. 12 $-\ln(1-\phi)$ vs $(V-V_{fb})^{1/2}$ plot for determination of various parameters related to photoactivity of Pb/0.1 wt% Pt oxide electrode

This space charge width, w, was calculated from the relation

$$w = \left[\frac{2\epsilon\epsilon_0(V - V_{fb})}{qN_d}\right]^{1/2} \tag{3}$$

using donor density and flat-band potential from the a.c. impedance study (Table 1).

From Table 2 it is clear that the absorption co-efficient for different monochromatic radiation and space charge width is higher for pure lead oxide. This suggests that, because of the decrease in the unit cell dimension of lead oxide (as revealed from XRD analysis), the absorption co-efficient of light is affected. Moreover, this contraction of the cell may also be preventing the creation of a larger space charge width with lead oxide obtained with Pb-Pt alloy. This behavior also supports the fact that incorporation of platinum increases the donor density, which in turn is expected to decrease the space charge width. Similar behavior was reported with Pb-Sn and Pb-In alloys [10, 11].

This study suggests that, with α-PbO, controlling the oxygen deficiency alone cannot increase the photoactivity of the film, especially when lead is present in the back of the lead oxide. Doping of the lead oxide film should be done such that, without affecting the stoichiometry of lead oxide, the donor concentration is increased. This is a difficult task to achieve.

Conclusions

It can be concluded that better efficiency could be achieved if we could modify the surface of α-PbO without affecting the orientation of the (110) plane. From this study, it was also confirmed that the (110) plane is mainly responsible for the photoactivity. Gartner analysis suggested that Pt doping in α-PbO has not significantly increased the photoactivity of the lead oxide film.

Table 2 Parameters related to photoactivity of the oxide photoanode. t is the time of anodization, λ is the wavelength of incident light, L is the diffusion length of the minority carrier, w is the space charge width, α is the absorption coefficient of the oxide and α^{-1} is the penetration depth

t (min)	λ (nm)	α (cm^{-1})	α^{-1} (Å)	w (Å)	L (Å)
		Pure lead oxide			
20	550	2503	39,947	6311	8319
20	530	3493	28,622	6311	9260
20	500	10,265	9741	6311	4576
20	480	13,652	7324	6311	3559
20	460	10,799	9259	6311	3510
		Pb/0.1 wt% Pt oxide			
20	550	6300	15,871	1432	2360
20	530	6556	15,251	1432	3659
20	500	7032	14,219	1432	6584
20	480	13,022	7679	1432	3807
20	460	15,390	6497	1432	1690

References

1. Pavlov D, Iordanov N (1970) J Electrochem Soc 117: 1103
2. Pavlov D, Poulieff CN, Klaja E, Iornadov N (1969) J Electrochem Soc 116: 316
3. Veluchamy P, Sharon M, Kumar D (1991) J Electronal Chem 315: 293
4. Veluchamy P, Sharon M, Minoura H, Ichilhashi Y, Basavaswaran K (1993) J Electroanal Chem 344: 73
5. Veluchamy P, Sharon M (1993) J Electroanal Chem 361: 261
6. Veluchamy P, Sharon M (1994) J Electroanal Chem 365: 179
7. Mukhopadhyay I, Raghavan MSS, Sharon M, Minoura H, Veluchamy P (1994) J Electroanal Chem 379: 531
8. Veluchamy P, Sharon M, Shimizu M, Minoura H (1994) J Electroanal Chem 371: 205
9. Veluchamy P, Minoura H (1995) J Electrochem Soc 142: 1799
10. Mukhopadhyay I, Sharon M, Veluchamy P, Minoura H (1996) J Electroanal Chem 401: 139
11. Mukhopadhyay I, Ghosh S, Sharon M Solar Energy Materials and Solar Cells (in press)
12. Qinglin Li, Zhengshi Chen, Xinhua Zheng, Zhensheng Jin (1992) J Phys Chem 96: 5959
13. JCPDS Power Diffraction File Cards (1987) 5-561 (α-PbO), 5-570 (β-PbO), 4-686 (Pb) and 37-517 (α-PbO_2), ASTM, Philadelphia, PA
14. Chen S, Russak MA, Witzke H, Reichman J, Dep SK (1979) US Patent No. 4172925
15. Hodes G (1983) In: Gratzel M (ed) Energy resources through photochemistry and catalysis. Academic Press, New York, ch 13
16. Bullock KR (1987) J Electroanal Chem 222: 347
17. Taylor JA, Perry DL (1984) J Vac Sci technol A 2: 771
18. Pederson LR (1982) J Electron Spect Relat Phenom 28: 203
19. Chadwick D, Christe AB (1980) J Chem Soc, Faraday Trans II 76: 267
20. Nagasubramanian G, Wheller BL, Hope GA, Bard AJ (1983) J Electrochem Soc 130: 385
21. Gartner WW (1959) Phys Rev 116: 84
22. Bulter MA (1977) J Appl Phys 48: 1914
23. Bullock KR, Trischan GM, Burrow RG (1983) J Electrochem Soc 130: 1283